An Astrometric Measurement of Physical Binary WDS 10382+2636 STF1454 Using Speckle Interferometry

Heinz Vahlbruch [1], Mary Kovic [2], Pat Boyce [3], Grady Boyce [3]

[1] Boyce Research Initiatives and Education Foundation (BRIEF), San Diego California; hello@heinzvahlbruch.com
[2] University of California San Diego
[3] Boyce Research Initiatives and Education Foundation (BRIEF), San Diego California

Abstract: Known binary star system 10382+2636 STF 1454 (HD 92049) was observed on March 28, 2023 using the BARO Planewave Corrected Dahl-Kirkham (CDK) 17 telescope at the Boyce Astro Research Observatory. Speckle Interferometry, a method to resolve the separation of star systems with especially small separations, was used on our target system with a last-recorded separation of 1.296''. The software N.I.N.A. (Berg) was used to obtain images of WDS 10382+2636 using this imaging technique, and Speckle Toolbox (STB) 1.16 was used to perform autocorrelation and bi-spectrum analysis on this system. The mean position angle and standard deviation was 5.313° ± 0.391°, the mean separation and standard deviation was 1.207'' ± 0.0208'', and the mean delta magnitude and standard deviation was 1.928 ± 0.166.

1. Introduction

1.1 System Selection

When choosing potential targets, we used the following criteria to search the Washington Double Star Catalog (Mason, B.) through the website Stelle Doppie (Stelle Doppie): We limited our search to stars with a separation angle of less than 5'' between them, and magnitudes of 11 or brighter. And because our observations took place in the Northern Hemisphere and must be in the sky above 30 degrees at 8:00 PM PT, we narrowed down our search to stars with a right ascension between 0 and 10 and declination of 25 or greater. We were also interested in neglected doubles (meaning systems that have not been observed in more than 10 years) and stars that already have orbital data with a grade of 5, Figure 1. STF 1454 met all our search requirements and was chosen to be our target system.

1.2 Hypothesis

Because our system is a known binary, our goals of this research will be to establish the precision and accuracy of measurements of double stars made by speckle interferometry and verify the accuracy of the ephemeris. Our research will similarly focus on obtaining high resolution measurements of binary stars using sensitive detectors. We can also contribute to a better knowledge of the apparent relative motion of long-period binaries such as this one so that very accurate orbits could be determined in the future. This could mean that fundamental parameters such as stellar masses could be inferred from them.

1.3 STF 1454

STF 1454 is a certain physical double star and possible multi star system. It has an especially long orbital period of 1160.0744 years (Izmailov, 2019) and has unknown data for the B star's parallax and distance (Simbad). Figure 2 shows our system and its components in an image collected using Aladin 10 (Bonnarel, F.), Figure 2. The small separation between the components makes STF 1454 difficult to capture using traditional imaging techniques.

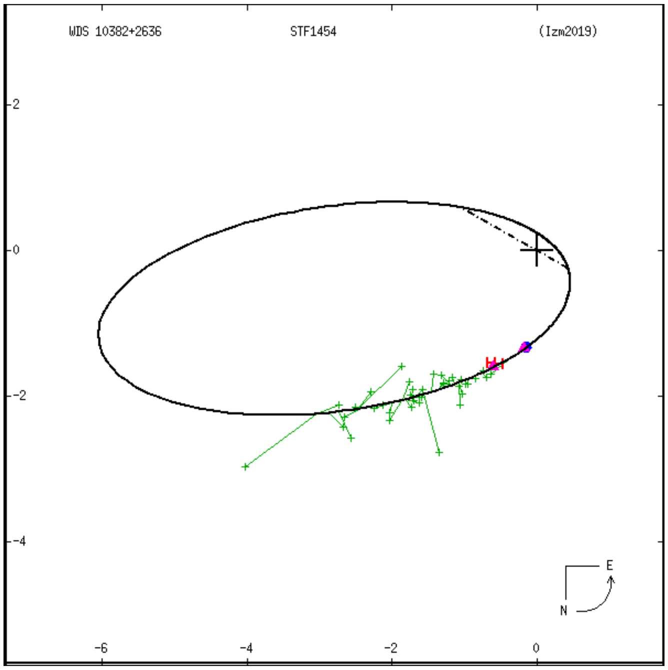

Figure 1: The projected orbital trajectory of STF 1454 obtained from the request for WDS historical data provided by the USNO (Mason, B.)

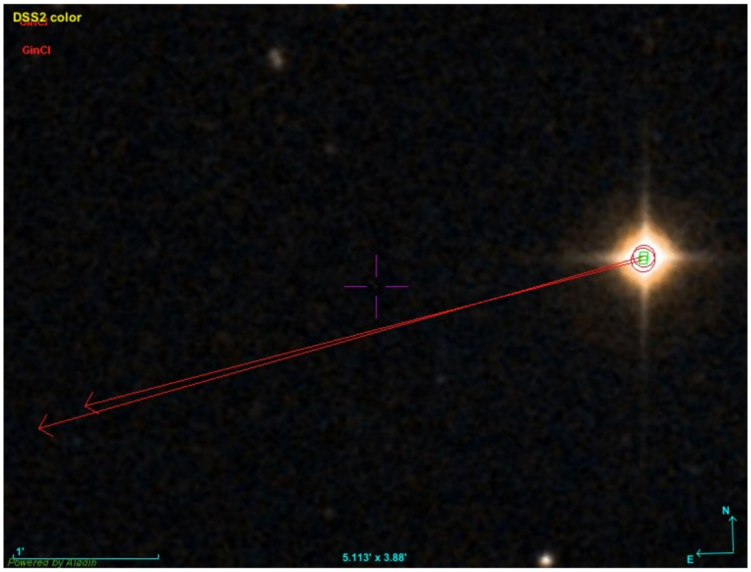

Figure 2: Image of STF 1454 obtained using DSS2and Simbad filters on Aladin 10 (Bonnarel, F.)

First discovered in 1830, and last observed in 2016, this system has had just a smattering of observations over nearly two centuries. The last measured separation is just above 1’’, both stars are brighter than magnitude 10 and their delta magnitude is less than 2.5.

Although first observed by Wilhelm von Struve, observations not recorded in the WDS historical catalog have been published in other papers. René Gili, Jean-Louis Prieur, Jean-Pierre Rivet, Farrokh

Vakili, Marco Scardia, et al. uses PISCO2, a speckle camera that was specifically designed for its telescope (René Gili),(Marco Scardia).

We can take guidance from the methods used in these papers even if we do not use the same equipment by observing their objectives and trying to reach similar quality of measurements they have for our system or compare our setup and results to theirs.

2. Equipment and Methods

Because our system has an apparent separation of less than 5’’, we decided to use Speckle Interferometry for our observation to reduce atmospheric distortion, an unwanted interferences present when observing double stars with small separations. Speckle Interferometry requires many images of the target system as well as an appropriate number of images for the reference star, which are used to complete the Fourier transform (Labeyrie).

On March 28, 2023 (Epoch 2023.24), we observed the system with the BARO Planewave Corrected Dahl-Kirkham (CDK) 17 telescope, Figure 3, which has a focal ratio of f/6.8 and a focal length of 2939mm, mounted on an equatorial Planewave L-500 mount. We used a ZWO ASI 1600 monochrome CMOS 16-megapixel camera with a pixel image scale of 0.107’’, set up with a Sloan r filter and a 2.5X Barlow, resulting in a focal ratio of f/17 and focal length of 7348mm .

The telescope has a FOV of about 8.3’’x6.3’’, which is usually too small to contain the 10 stars to develop a plate-solving solution. Therefore, we pointed the telescope to a nearby open cluster and took 10 long exposure images. We measured the camera angle and plate scale (arcseconds per image pixel) for each of these calibration images. Then we calculated the mean values to use in Speckle Tool Box (Harshaw, R., Rowe, D., and Genet, R.). The software used to capture the images was the image acquisition software N.I.N.A. (Nighttime Imaging ‘N’ Astronomy) (Berg) with a special N.I.N.A. Speckle Interferometry plugin developed by Nick Hardy and Leon Bewersdorff (Hardy).

During the image acquisition run on our target system, three sets of 1000 images each were taken with different exposure times. We took 300 images of the reference star for each exposure time. Due to the large number of images and to keep the data volume manageable, camera binning was set to 1x1, and the images were cropped to 256px by 256px during STB bispectrum phase reduction processing. All images were taken in the FITS file format.

Figure 3: Image of the BARO telescope

We used the software Speckle Toolbox 1.16 (STB) to obtain measurements for the values of Theta, Rho, and delta magnitude. Using STB, FITS cubes were created for the different exposure times from the target and reference star images, Figure 4. Each FITS cube was processed into a 4-D array of Correlations, a so-called BSP-file, Figure 5.

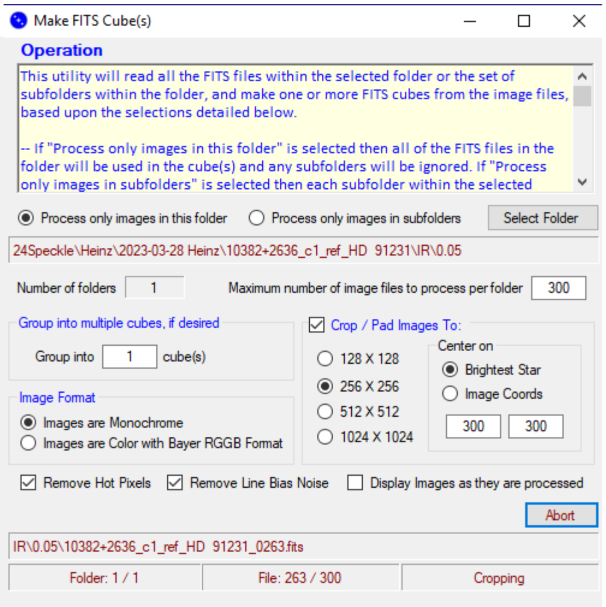

This utility will read all the FITS files within the selected folder or the set of subfolders within the folder, and make one or more FITS cubes from the image files, based upon the selections detailed below.

-- If "Process only images in this folder" is selected then all of the FITS files in the folder will be used in the cube(s) and any subfolders will be ignored. If "Process only images in subfolders" is selected then each subfolder within the selected

● Process only images in this folder ○ Process only images in subfolders

24Speckle\Heinz\2023-03-28 Heinz\10382+2636_c1_ref_HD 91231\IR\0.05

Number of folders 1

Maximum number of image files to process per folder 300

Group into multiple cubes, if desired

Group into 1 cube(s)

Image Format

● Images are Monochrome
○ Images are Color with Bayer RGGB Format

☑ Crop / Pad Images To:

○ 128 X 128
● 256 X 256
○ 512 X 512
○ 1024 X 1024

Center on

● Brightest Star
○ Image Coords
300 300

☑ Remove Hot Pixels ☑ Remove Line Bias Noise ☐ Display Images as they are processed

IR\0.05\10382+2636_c1_ref_HD 91231_0263.fits

Folder: 1 / 1 File: 263 / 300 Cropping

Figure 4: Specifications used for creating FITS cubes

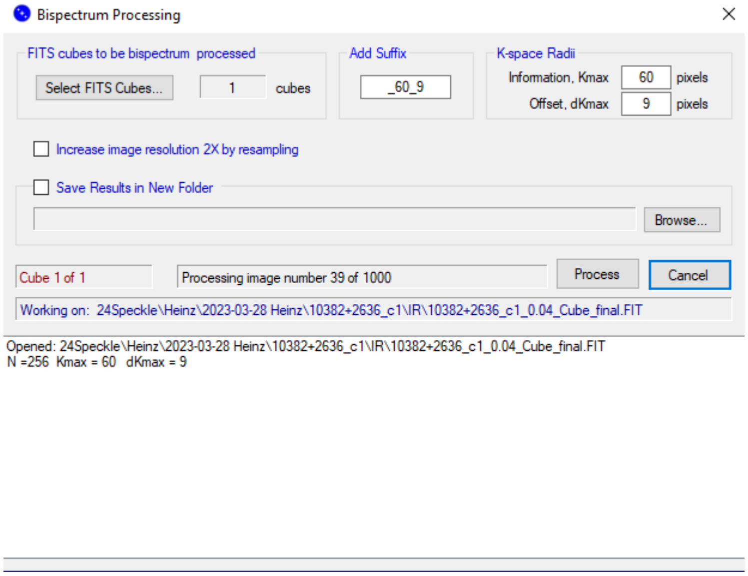

FITS cubes to be bispectrum processed

1 cubes

Add Suffix _60_9

K-space Radii

Information, Kmax 60 pixels

Offset, dKmax 9 pixels

☐ Increase image resolution 2X by resampling

☐ Save Results in New Folder

Cube 1 of 1

Processing image number 39 of 1000

Working on: 24Speckle\Heinz\2023-03-28 Heinz\10382+2636_c1\IR\10382+2636_c1_0.04_Cube_final.FIT

Opened: 24Speckle\Heinz\2023-03-28 Heinz\10382+2636_c1\IR\10382+2636_c1_0.04_Cube_final.FIT
N =256 Kmax = 60 dKmax = 9

Figure 5: Specifications used for creating BSP-files

Bispectrum phase reconstruction was performed in independent sets with ten measurements for each exposure time in each set. We decided to use this approach to get a reasonable number of measurements and to rule out any data outliers. Our process, two members working on BSP-files for three different exposure times and taking 10 measurements for each, resulted in a total of 60 measurements for Theta, Rho, and delta magnitude.

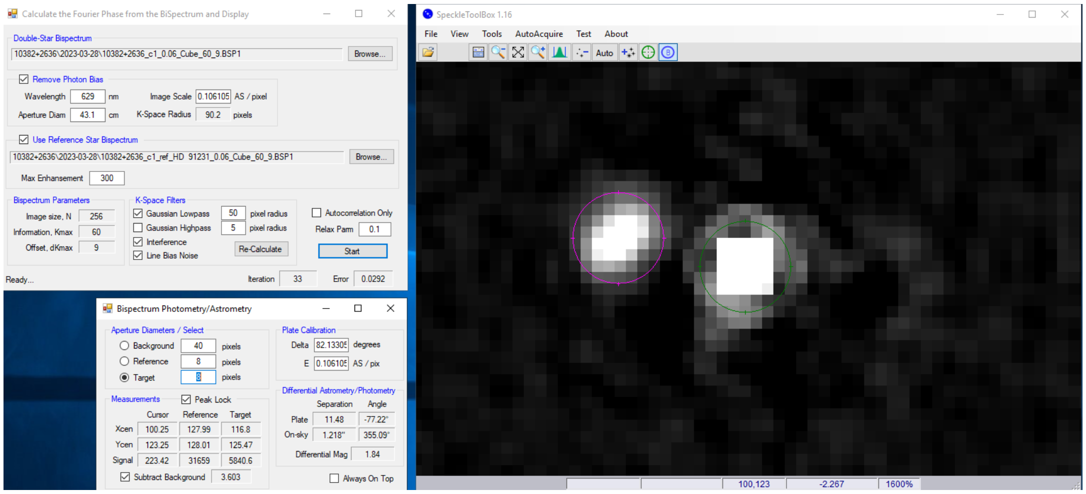

Calculate the Fourier Phase from the BiSpectrum and Display

Double-Star Bispectrum: 10382+2636\2023-03-28\10382+2636_c1_0.06_Cube_60_9.BSP1

☑ Remove Photon Bias
Wavelength 629 nm
Image Scale 0.106105 AS / pixel
Aperture Diam 43.1 cm
K-Space Radius 90.2 pixels

☑ Use Reference Star Bispectrum: 10382+2636\2023-03-28\10382+2636_c1_ref_HD 91231_0.06_Cube_60_9.BSP1
Max Enhansement 300

Bispectrum Parameters
Image size, N 256
Information, Kmax 60
Offset, dKmax 9

K-Space Filters
☑ Gaussian Lowpass 50 pixel radius
☐ Gaussian Highpass 5 pixel radius
☑ Interference
☑ Line Bias Noise

☐ Autocorrelation Only
Relax Parm 0.1

Ready... Iteration 33 Error 0.0292

Bispectrum Photometry/Astrometry

Aperture Diameters / Select
○ Background 40 pixels
○ Reference 8 pixels
● Target 8 pixels

Measurements ☑ Peak Lock

	Cursor	Reference	Target
Xcen	100.25	127.99	116.8
Ycen	123.25	128.01	125.47
Signal	223.42	31659	5840.6

☑ Subtract Background 3.603

Plate Calibration
Delta 82.13305 degrees
E 0.106105 AS / pix

Differential Astrometry/Photometry

	Separation	Angle
Plate	11.48	-77.22°
On-sky	1.218"	355.09°

Differential Mag 1.84

☐ Always On Top

Figure 6: STB panels with specifications for the phase reconstruction and astrometry

The On Sky Position Angle taken from STB was converted to the real Position Angle in respect of the orientation of the camera during the image acquisition.

3. Data

Table 1 shows the details of our image acquisition process and how many different measurements (phase reconstructions in STB) were performed.

Table 1. Data table showing observation dates, exposure times and used equipment.

WDS 10382+2636 STF1454							
Equipment	Epoch	Date Local	Date UTC	Exposure Time	Target Image Count	Reference Star Image Count	Number of Measurements
BARO Sloan r	2023.24	3/28/2023	3/29/2023	0.04	1000	300	20
	2023.24	3/28/2023	3/29/2023	0.05	1000	300	20
	2023.24	3/28/2023	3/29/2023	0.06	1000	300	20

We calculated mean values, Standard Deviation, and Standard Error of the Mean for Theta, Rho, and delta magnitude using all 60 measured values for Theta, Rho, and delta magnitude.

The following Table 2 shows our results in comparison to latest historical WDS (Mason, B.) measurements and predicted ephemeris from the Sixth Catalog of Orbits (Matson).

Table 2. Results for our and historical measurements and predicted values.

WDS 10382+2636 STF1454 Measurements				
Epoch	Measurement	Theta (degrees)	Rho (arcseconds)	Delta magnitude (sloan r)
2023.24	Mean	5.3125	1.20699	1.928067
	Standard Deviation	0.391003	0.020792	0.165652
	Standard Error of the Mean	0.050478	0.002684	0.021386

2016.0	WDS - Last Observed	2.71	1.30124	1.215
2023.24	Sixth Catalog of Orbits - Ephemeris Izmailov, 2019	6.588	1.10268	N/A

4. Discussion

We combined all our 60 measurement records into a single data table and performed a statistical data analysis to evaluate our data. This was done to see whether our measurements were well distributed over a range of values or whether there were any outliers or other measurement issues. We used the Python programming language (Van Rossum) and the pandas (McKinney), NumPy (Harris), Matplotlib (J. D. Hunter) and Seaborn (Waskom) libraries to build our own data analysis solution in a JupyterLab notebook. Several data distribution plots were created to compare measurements for Theta and Rho taken by the two members (Figure 7), data distributions for Theta (Figure 8, 11), Rho (Figures 9, 12) and delta magnitude (Figures 10, 13).

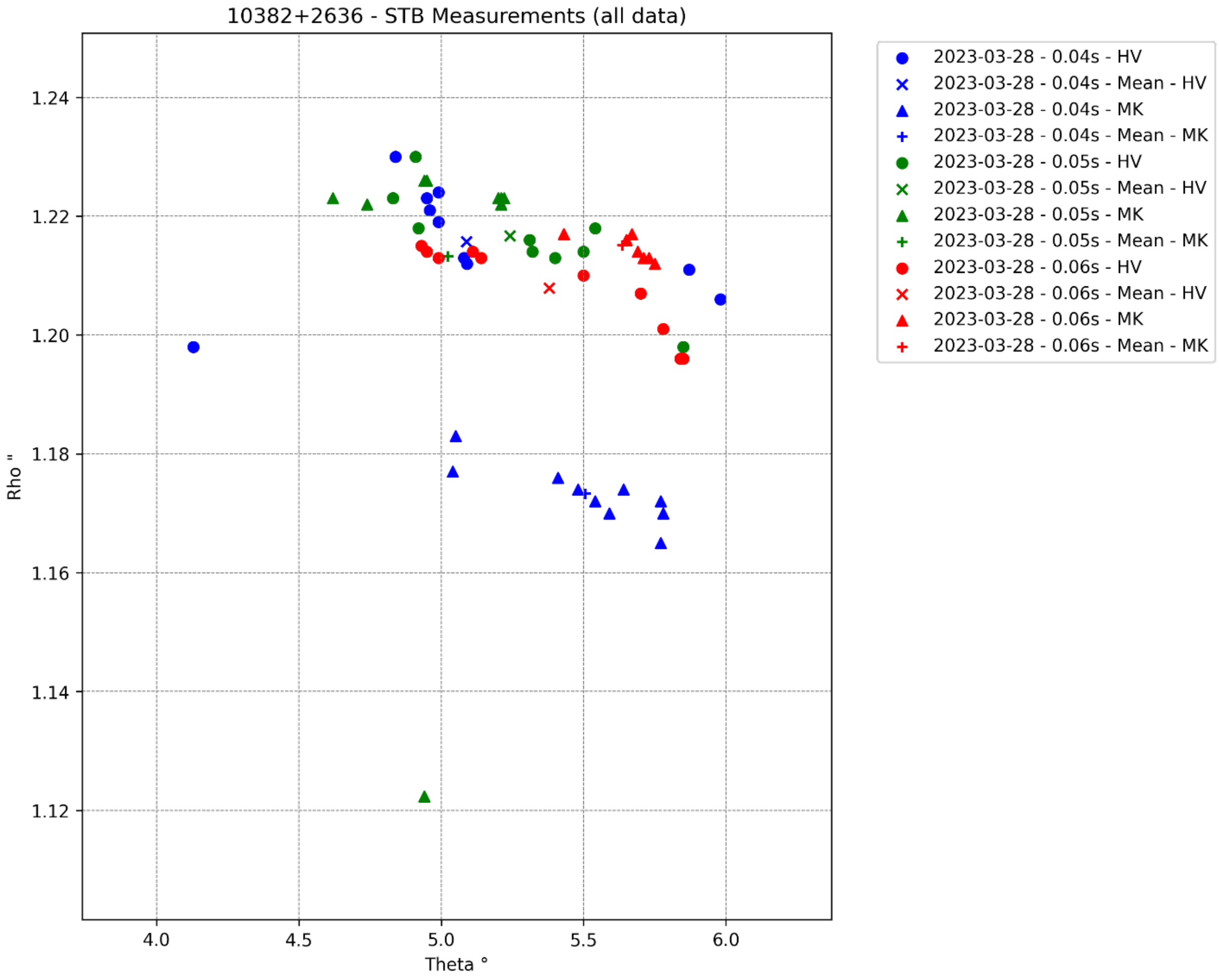

Figure 7: Plot showing measurements for Theta, Rho by members HV, MK

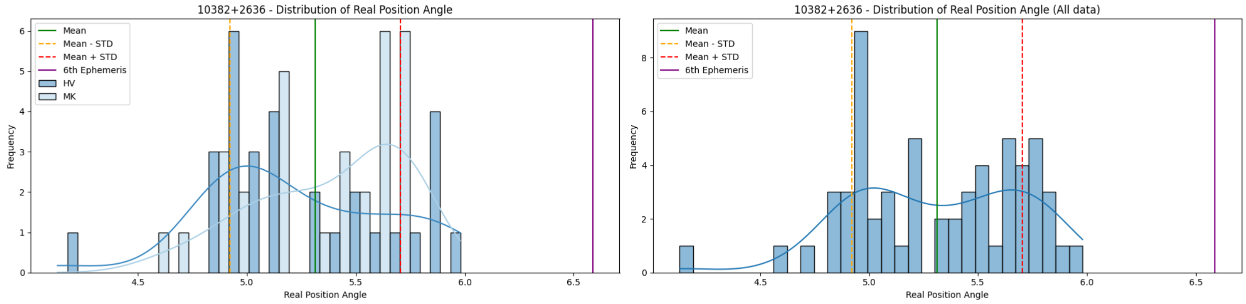

Figure 8: Plot showing measurement value distribution for Theta

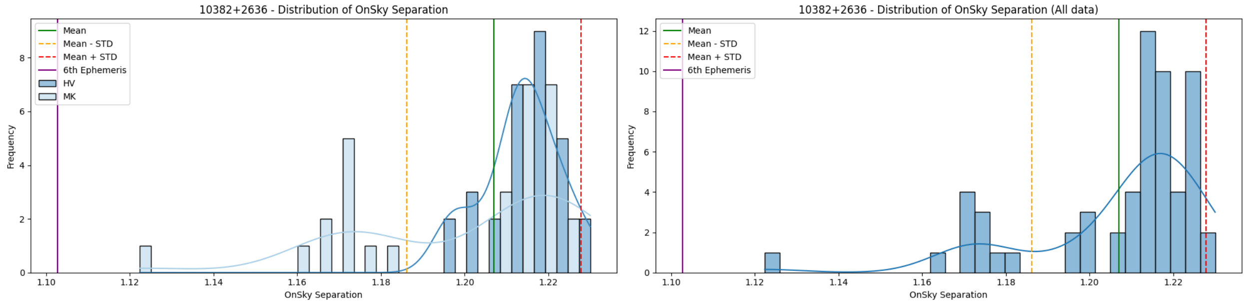

Figure 9: Plot showing measurement value distribution for Rho

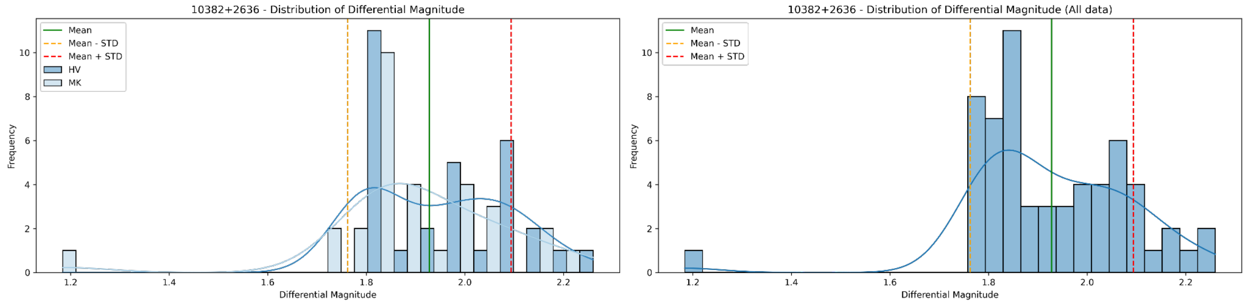

Figure 10: Plot showing measurement value distribution for delta magnitude

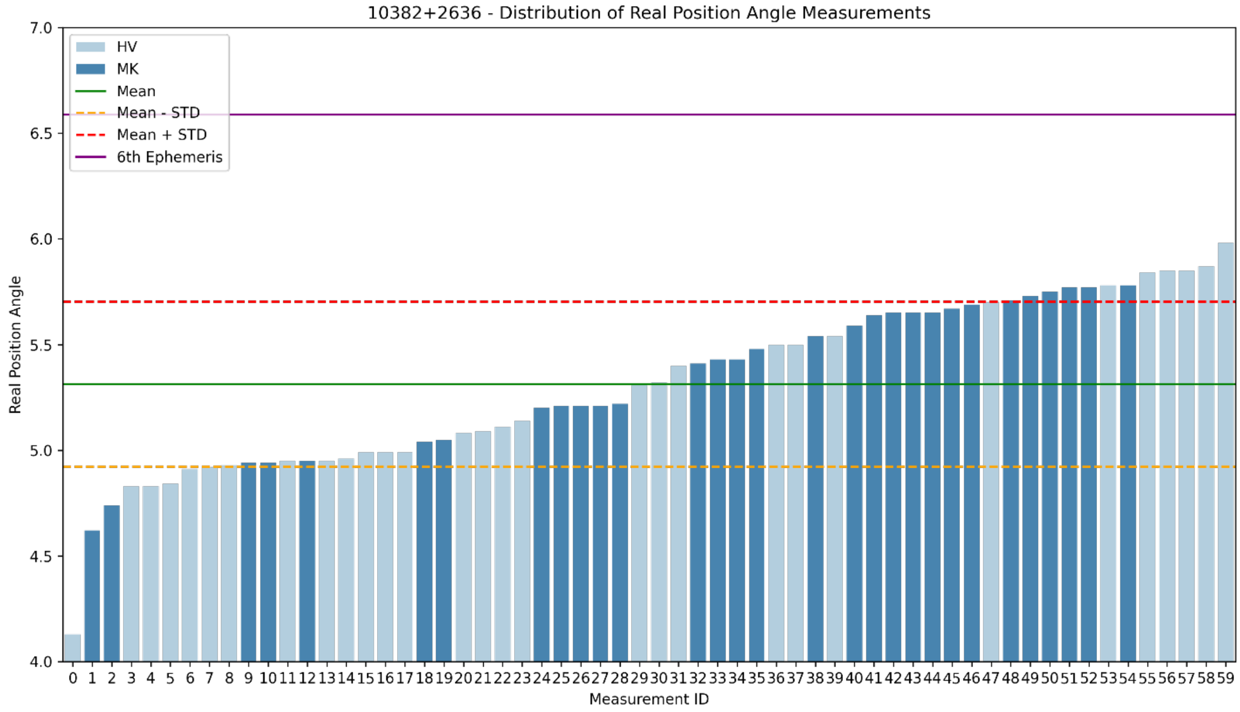

Figure 11: Plot showing measurement value distribution for Theta

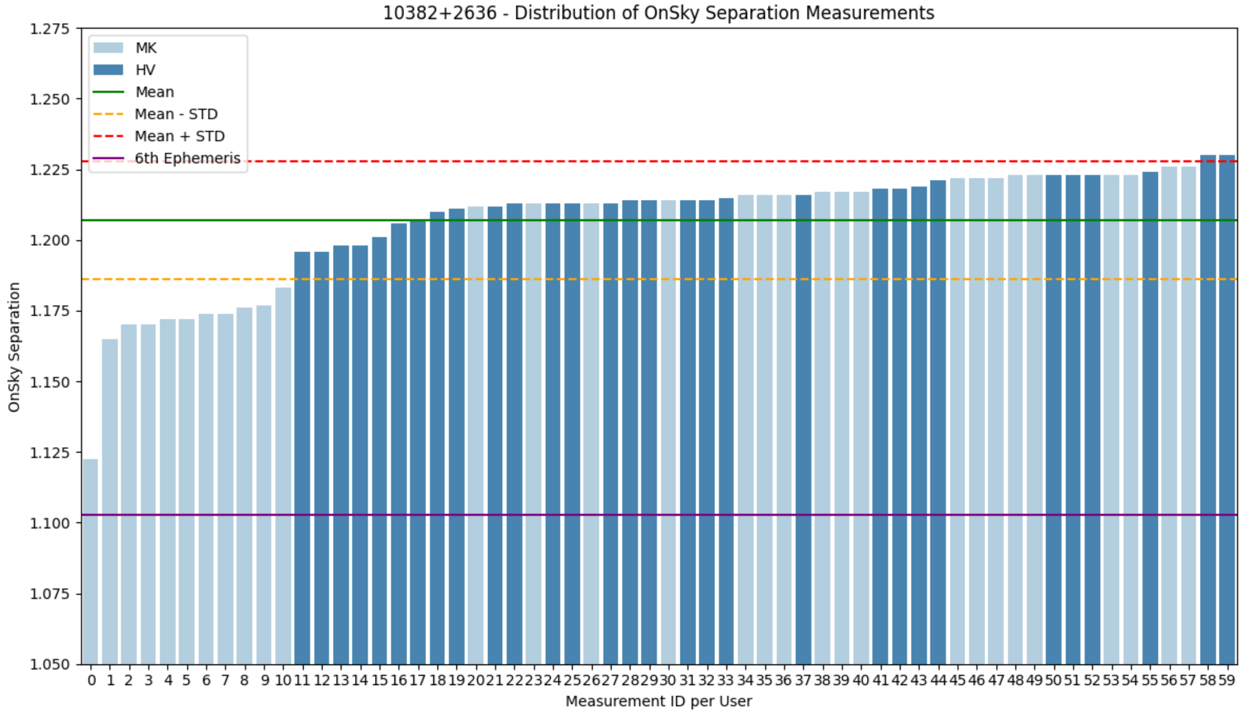

Figure 12: Plot showing measurement value distribution for Rho

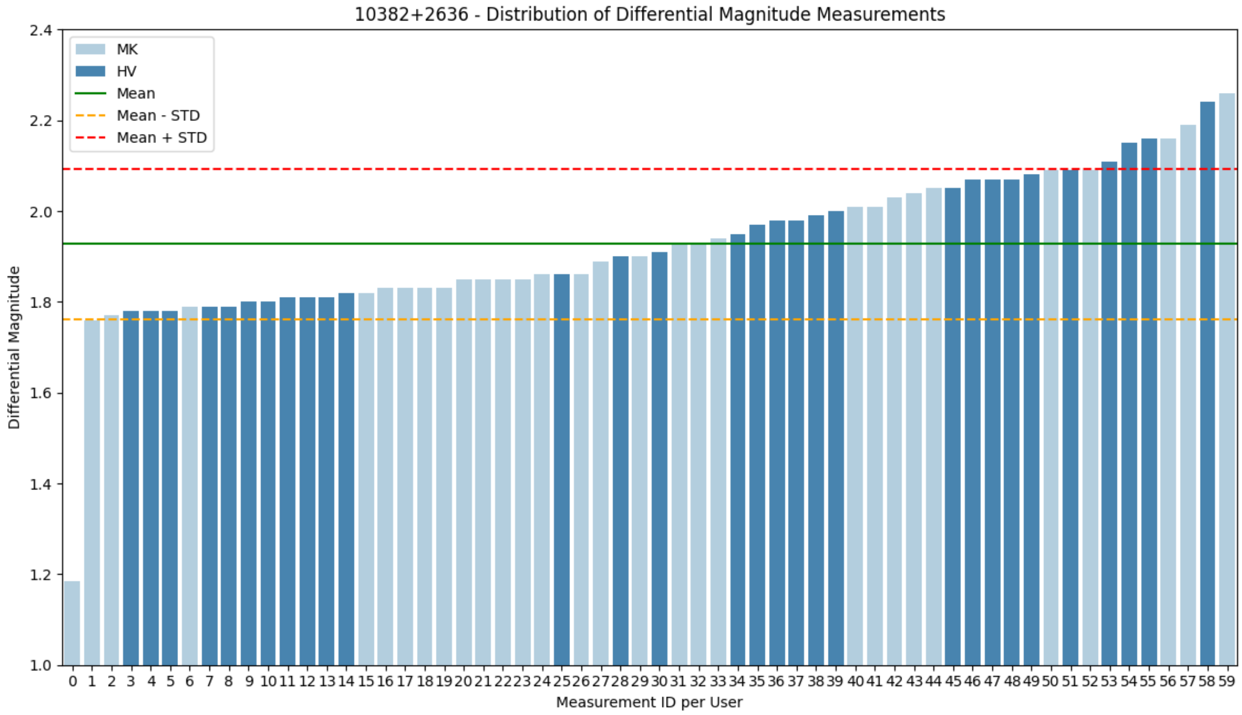

Figure 13: Plot showing measurement value distribution for delta magnitude

Since the plot on figure 7 shows a significant difference for the measured values of Rho for the 40ms observation measured by user MK and the plots on figures 8, 9, and 10 do not show a clear normal distribution over all data, but normal distributions over the data per user, we wanted to analyze how well our measurements fit into a normal distribution by using the empirical rule. In particular, the empirical rule predicts that in normal distributions, 68% of observations fall within the first standard deviation (μ ± σ), 95% within the first two standard deviations (μ ± 2σ), and 99.7% within the first three standard deviations (μ ± 3σ) of the mean. We calculated the percentages of our measurements for Theta, Rho, and Delta Magnitude being in the ranges of +/- 1 STD (Table 3), +/- 2 STD (Table 4), and +/- 3 STD respectively (Table 5).

Table 3. Data table showing measurement value distributions for Theta, Rho, and Delta Magnitude for +/- 1 STD.

	Theta	Rho	Delta Magnitude
Total Measurements	60	60	60
Mean μ	5.3125	1.20699	1.928067
STD σ	0.391003	0.020792	0.165652
μ - σ	4.921497	1.186198	1.762415
μ + σ	5.7035029	1.227782	2.093719
Measurements between μ ± σ	40	47	51
Percentage between μ ± σ	66.66 %	78.33 %	85.0 %
Target percentage	68 %	68 %	68 %
Percentage Difference	-1.34 %	+10.33 %	+17 %

Table 4. Data table showing measurement value distributions for Theta, Rho, and Delta Magnitude for +/- 2 STD.

	Theta	Rho	Delta Magnitude
Total Measurements	60	60	60
Mean μ	5.3125	1.20699	1.928067
STD σ	0.391003	0.020792	0.165652
μ - 2σ	4.530494	1.165406	1.596763
μ + 2σ	6.094506	1.248574	2.259371
Measurements between μ ± 2σ	59	58	58
Percentage between μ ± 2σ	98.33 %	96.66 %	96.66 %
Target percentage	95 %	95 %	95 %
Percentage Difference	+3.33 %	+1.66 %	+1.66 %

Table 5. Data table showing measurement value distributions for Theta, Rho, and Delta Magnitude for +/- 3 STD.

	Theta	Rho	Delta Magnitude
Total Measurements	60	60	60
Mean μ	5.3125	1.20699	1.928067
STD σ	0.391003	0.020792	0.165652
μ - 3σ	4.139491	1.144614	1.431111
μ + 3σ	6.485509	1.269366	2.425023
Measurements between μ ± 3σ	59	59	59
Percentage between μ ± 3σ	98.33 %	98.33 %	98.33 %
Target percentage	99.7 %	99.7 %	99.7 %
Percentage Difference	-1.37 %	-1.37 %	-1.37 %

The aberration in value for Rho of our measurements for the 40ms observation measured by user MK represents 1/6 or 17% of the sample size (Figure 7). However, those measured values still show a similar distribution range as the other 5/6 or 83% of all measured values for Rho. We therefore decided to include the 40ms measurements from user MK into our sample, as the overall effect for the results for Rho won't be noticeable.

The analysis for our measurements meeting the empirical rule shows a minimal shortage of -1.37 % for Theta in the +/- 1 STD range (Table 3) and a minimal shortage of -1.37 % for Theta, Rho, and Delta Magnitude in the +/- 3 STD range (Table 5). We suppose the small sample size of 60 to be the reason for the minimal differences and suppose our measurements to be distributed normally.

Based on our data table, the final mean values, Standard Deviation, and Standard Error of the Mean for Theta, Rho, and delta magnitude were calculated using our Python solution to be compared to the proposed ephemeris from the Sixth Catalog of Orbits of Visual Binary Stars (Matson) (Table 6).

Table 6. Sixth Catalog of Orbits of Visual Binary Stars: Ephemerides.

WDS	Name	Grade	Reference	Year	Theta	Rho
10382+2636	STF1454	5	Izm2019	2021.0	4	1.142
				2022.0	5.1	1.125
				2023.0	6.3	1.107
				2024.0	7.5	1.089
				2025.0	8.7	1.07

We used a linear interpolation to find the proposed ephemeris for the given date of our observation (Bush, M.):

$$(1)\ y = y1 + a(y2 - y1)$$

where y is the ephemeris for Theta or Rho on the given date, $y1$ the ephemerid for a given year and $y2$ the year after it, and a the decimal value of the date falling between the given years.

Our observation date is 2023.24 and it follows that a is 0.24, $y1$ and $y2$ are the ephemerides for the years 2023 and 2024. Using the values for the proposed ephemerides provided by the Sixth Catalog of Orbits of Visual Binary Stars (Matson), it is found that the interpolated predicted ephemeris for our system on our observation date is Theta = 6.588° and Rho = 1.10268''.

The difference between the observed and the predicted interpolated values is 1.2755° or 3.26 σ and -0.10431'' or 5.02 σ for Theta and Rho respectively.

WDS Historical Data shows only two recent measurements done with Speckle for 2010.222 and 2016.338. We wanted to put our Speckle results in perspective and compared them with data from other recent Speckle observation programs (René Gili) where results for our system were found for 2011.26 and 2012.24 (Table 7). The results found for 2011.26 and 2012.24 are taken from a paper published in 2022 (René Gili) and are not yet distributed with data by WDS.

Table 7. Results from Measurements of visual binaries with PISCO2 at the Nice 76-cm refractor in 2011-2012 (René Gili).

WDS	10382+2636	
Name	STF1454	
Notes	Izm2019	
Epoch	2011.266	2012.246
Bin.	1	1
ρ ('')	1.367	1.342
σρ ('')	0.007	0.007
θ (°)	354.0*	354.7*
σθ (°)	0.3	0.3
Δm	-	-
Orbit	-	-
Δρ(O−C) ('')	0.05	-0.8

Δθ(O−C) (°)	0.06	-0.7

* The superscript ∗ indicates that the position angle θ could be determined without the 180◦ ambiguity.

We used the Binary Orbit Tool of Speckle Toolbox 10.03 (STB10) to plot an orbital solution for our system based on the data provided by WDS. We added the two results from 2011.26 and 2012.24 (René Gili) as well as our calculated results to the data for the plot.

Figure 14 shows our result added to an orbital solution in combination with historical data from the WDS (Mason, B.), other recent Speckle observation results, and predicted ephemeris from the Sixth Catalog of Orbits (Matson).

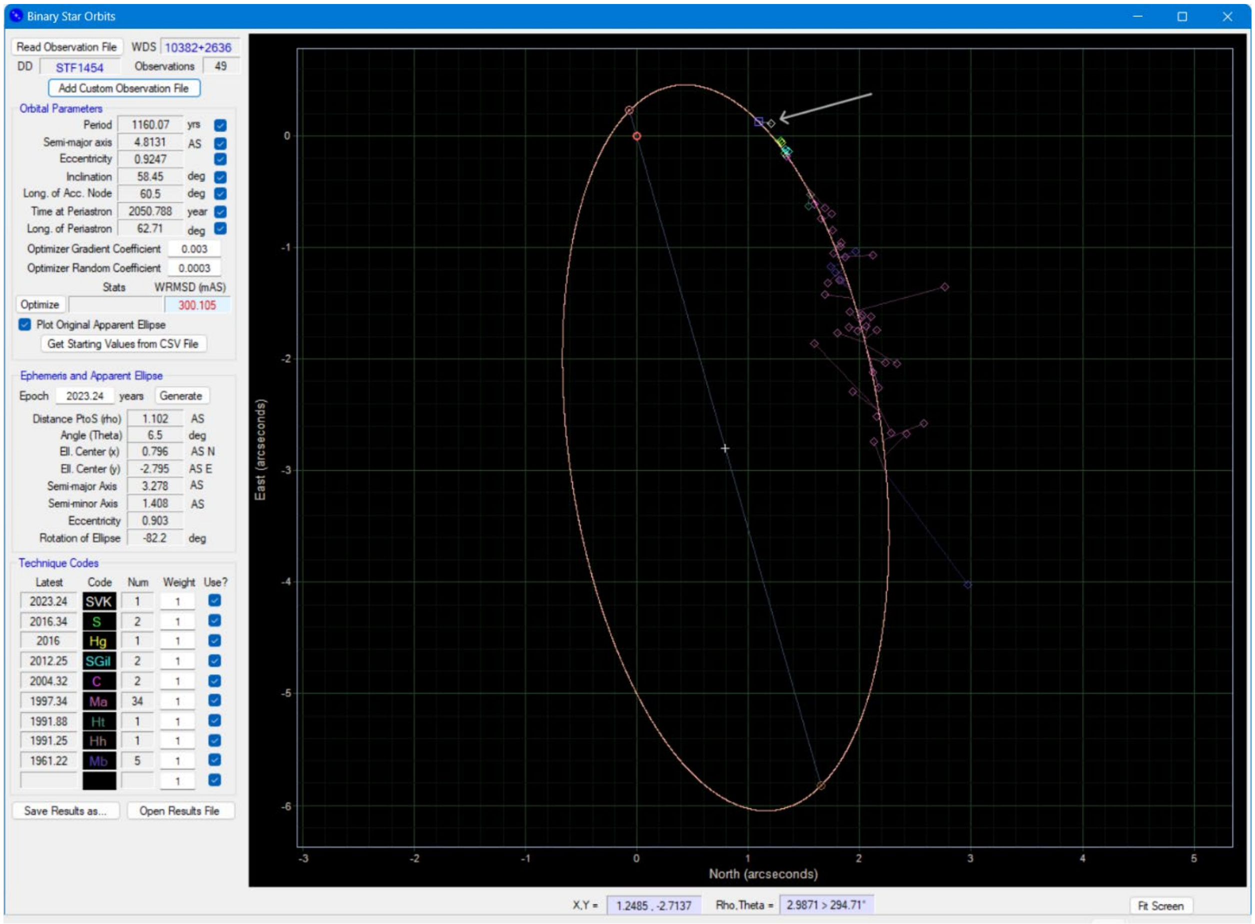

WDS 10382+2636
DD STF1454
Observations 49

Period 1160.07 yrs ☑
Semi-major axis 4.8131 AS ☑
Eccentricity 0.9247 ☑
Inclination 58.45 deg ☑
Long. of Acc. Node 60.5 deg ☑
Time at Periastron 2050.788 year ☑
Long. of Periastron 62.71 deg ☑
Optimizer Gradient Coefficient 0.003
Optimizer Random Coefficient 0.0003
Stats
WRMSD (mAS) 300.105
☑ Plot Original Apparent Ellipse

Epoch 2023.24 years
Distance PtoS (rho) 1.102 AS
Angle (Theta) 6.5 deg
Ell. Center (x) 0.796 AS N
Ell. Center (y) -2.795 AS E
Semi-major Axis 3.278 AS
Semi-minor Axis 1.408 AS
Eccentricity 0.903
Rotation of Ellipse -82.2 deg

Latest	Code	Num	Weight	Use?
2023.24	SVK	1	1	☑
2016.34	S	2	1	☑
2016	Hg	1	1	☑
2012.25	SGil	2	1	☑
2004.32	C	2	1	☑
1997.34	Ma	34	1	☑
1991.88	Ht	1	1	☑
1991.25	Hh	1	1	☑
1961.22	Mb	5	1	☑
			1	☑

X,Y = 1.2485 , -2.7137
Rho,Theta = 2.9871 > 294.71°

Figure 14: STB showing orbital solution with historical data from WDS, recent Speckle observations and our results over all exposure times (arrow)

Figure 15 shows a part of the orbital solution in detail with a marker for the position of our star on our observation date 2023.24. The color-coded markers represent our measurement with the label SVK, historical data from the WDS (Mason, B.) with the labels S, Hg, C, and other recent Speckle observation results (René Gili) not yet provided by WDS with the label SGil.

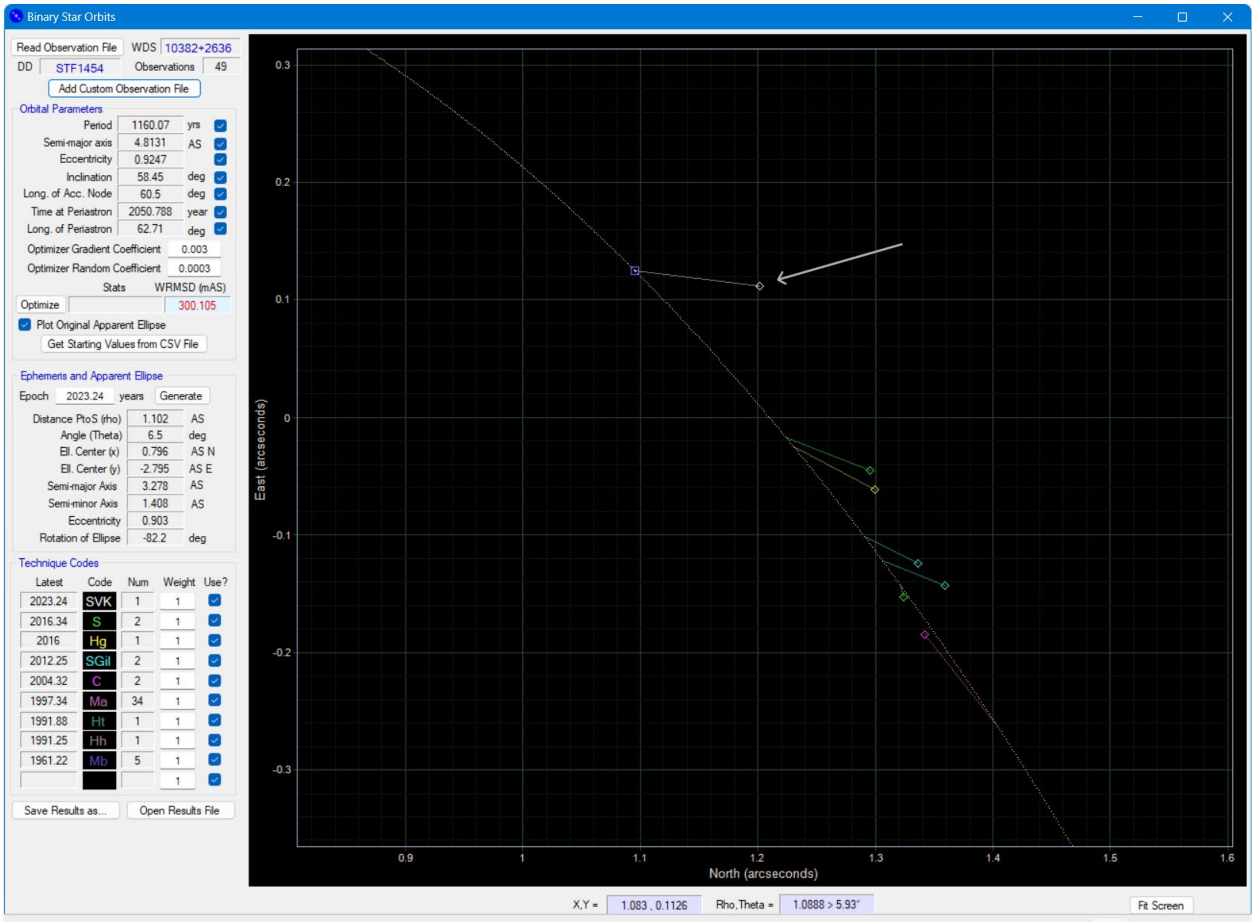

WDS 10382+2636
DD STF1454
Observations 49

Orbital Parameters

Period	1160.07	yrs	☑
Semi-major axis	4.8131	AS	☑
Eccentricity	0.9247		☑
Inclination	58.45	deg	☑
Long. of Acc. Node	60.5	deg	☑
Time at Periastron	2050.788	year	☑
Long. of Periastron	62.71	deg	☑

Optimizer Gradient Coefficient 0.003
Optimizer Random Coefficient 0.0003
Stats WRMSD (mAS) 300.105
☑ Plot Original Apparent Ellipse

Ephemeris and Apparent Ellipse

Epoch 2023.24 years

Distance PtoS (rho)	1.102	AS
Angle (Theta)	6.5	deg
Ell. Center (x)	0.796	AS N
Ell. Center (y)	-2.795	AS E
Semi-major Axis	3.278	AS
Semi-minor Axis	1.408	AS
Eccentricity	0.903	
Rotation of Ellipse	-82.2	deg

Technique Codes

Latest	Code	Num	Weight	Use?
2023.24	SVK	1	1	☑
2016.34	S	2	1	☑
2016	Hg	1	1	☑
2012.25	SGil	2	1	☑
2004.32	C	2	1	☑
1997.34	Ma	34	1	☑
1991.88	Ht	1	1	☑
1991.25	Hh	1	1	☑
1961.22	Mb	5	1	☑
			1	☑

X,Y = 1.083 , 0.1126 Rho,Theta = 1.0888 > 5.93°

Figure 15: STB showing detail of orbital solution with historical data from WDS, recent Speckle observations and our results over all exposure times (arrow)

It is interesting to point out that the results from recent Speckle observations with the codes SVK, S, SGil, as well as the most recent GAIA observation from 2016.0 with code Hg, are significantly different to the proposed Sixth Catalog of Orbits (Matson) ephemerides. It is also interesting that the more recent an observation, the greater the error compared to the proposed ephemeris.

Conclusion

The results of this paper show that more accurate Speckle observations provide results with a high divergence especially for Theta from historical data and the predicted values described by the ephemeris data. The current orbital solution seems to be derived from historical data retrieved from visual observations, which may have a lower accuracy compared to data obtained with Speckle observations. We consider this system worthy of being observed again, since we cannot prove the current orbital solution. We recommend future observers to take more measurements of this system to extend the amount of accurate data points with the long-term goal of updating and improving the orbital solution for this system.

5. Acknowledgements

We would like to thank Dr. Rachel Matson for providing the historical data required for the analysis of STF 1454. The analysis of the images taken of this system was made possible through David Rowe's software Speckle Tool Box (STB). We would also like to acknowledge the Boyce Research Initiatives and

Education Foundation for the use of their telescope Boyce-Astro Research Observatory North (BARON) located at the Sierra Remote Observatory (SRO). Finally, we would like to thank Pat Boyce and Grady Boyce for providing the guidance and support required to complete this paper.

This research has made use of the Washington Double Star Catalog maintained at the U.S. Naval Observatory. This work has also made use of data from the European Space Agency (ESA) mission Gaia (https://www.cosmos.esa.int/gaia), processed by the Gaia Data Processing and Analysis Consortium (DPAC, https://www.cosmos.esa.int/web/gaia/dpac/consortium). Funding for the DPAC has been provided by national institutions, in particular the institutions participating in the Gaia Multilateral Agreement.

6. References

Berg, Stefan. N.I.N.A. - Nighttime Imaging 'N' Astronomy https://nighttime-imaging.eu/

Bonnarel, F., “The ALADIN interactive sky atlas. A reference tool for identification of astronomical sources”, Astronomy and Astrophysics Supplement Series, vol. 143, pp. 33–40, 2000. doi:10.1051/aas:2000331

Bush, M. (2018). Astrometry Observations of STF 1321AB. Journal of Double Star Observations, 14(1), 38-43

Hardy, N., Bewersdorff, L., Rowe, D., Genet, R., Wasson R., Armstrong, J., Dixon, S., Harris, M., Smith, T., Freed, R., McCudden, P., Rajkumar Inbanathan S., S., Davis, M., Giavarini, C., Snyder, R., Wholly, R., Calvin, M., Cotton, S., Carter, J., Terrazas, M., Christopher R., S., Kumar A., A., Naskath H., S., and Ronald Rabin A., M. 2023, Automated Speckle Interferometry of Known Binaries, Journal of Double Star Observations Vol 19 No 2

Harris, C.R., Millman, K.J., van der Walt, S.J. et al. Array programming with NumPy. Nature 585, 357–362 (2020). DOI: 10.1038/s41586-020-2649-2

Harshaw, R., Rowe, D., and Genet, R. (2017). The SpeckleToolBox: A Powerful Data Reduction Tool for CCD Astrometry. Journal of Double Star Observations, 13(1), 16.

Heintz, W.D. (1978) Double Stars. In: Geophysics and Astrophysics Monographs, Vol. 15, Springer, Dordrecht. https://doi.org/10.1007/978-94-009-9836-0

Izmailov, I.S. 2019 AstL 45 30I, Orbital elements from weighted solutions used when available (Table 2), unweighted elements (Table 1) used for remaining 29 systems.

J. D. Hunter, "Matplotlib: A 2D Graphics Environment", Computing in Science & Engineering, vol. 9, no. 3, pp. 90-95, 2007

Labeyrie, A. (1970). Attainment of Diffraction Limited Resolution in Large Telescopes by Fourier Analyzing Speckle Patterns in Star Images. Astronomy and Astrophysics, 6, 85.

Marco Scardia, Jean-pierre Rivet, Jean-Louis Prieur, Luigi Pansecchi, Robert Argyle, et al.. Speckle observations with PISCO in Calern (France): I. Astrometric measurements of visual binaries in 2015–2016. Astronomical Notes / Astronomische Nachrichten, Wiley-VCH Verlag, 2019, 000, ff10.1002/asna.201913642ff. ffhal-02357163

Mason, B., (2018). The Washington Double Star Catalog, Astrometry Department, U.S. Naval Observatory. http://ad.usno.navy.mil/wds/Webtextfiles/wdsnewframe2.html

Matson, Rachel, Stephen Williams, William Hartkopf, and Brian Mason. 2023. Sixth Catalog of Orbits of Visual Binary Stars. U.S. Naval Observatory, Washington, DC. http://www.astro.gsu.edu/wds/orb6.html

McKinney, Wes. Data structures for statistical computing in python, Proceedings of the 9th Python in Science Conference, Volume 445, 2010

NASA. (n.d.). Orbits & Ephemerides. NASA. https://ssd.jpl.nasa.gov/orbits.html

René Gili, Jean-Louis Prieur, Jean-pierre Rivet, Farrokh Vakili, Marco Scardia, et al.. Measurements of visual binaries with PISCO2 at the Nice 76-cm refractor in 2011-2012. Astronomical Notes / Astronomische Nachrichten, 2021, 342 (6), pp.865-889. ff10.1002/asna.202113985ff. ffhal-03290780v2

Stelle Doppie (2018). 15493+6032 HU 912. https://www.stelledoppie.it/index2.php?iddoppia=64003

T. B. Souza et al 2020 AJ 159 132 DOI 10.3847/1538-3881/ab6dcd

Van Rossum, G., & Drake, F. L. (2009). Python 3 Reference Manual. Scotts Valley, CA: CreateSpace

Waskom, M. L., (2021). seaborn: statistical data visualization. Journal of Open Source Software, 6(60), 3021, https://doi.org/10.21105/joss.03021